

Effect of Hydrofracking Fluid on Colloid Transport in the Unsaturated Zone

Wenjing Sang,^{†,‡,§} Cathelijne R. Stoof,[‡] Wei Zhang,^{||} Verónica L. Morales,[⊥] Bin Gao,[#] Robert W. Kay,[▲] Lin Liu,[#] Yalei Zhang,[§] and Tammo S. Steenhuis^{*,‡}

[†]National Engineering Research Center of Protected Agriculture, Institute of New Rural Development and [§]State Key Laboratory of Pollution Control and Resources Reuse, College of Environmental Science and Engineering, Tongji University, Shanghai 200092, China

[‡]Department of Biological and Environmental Engineering and [▲]Department of Earth and Atmospheric Sciences, Cornell University, Ithaca, New York 14853, United States

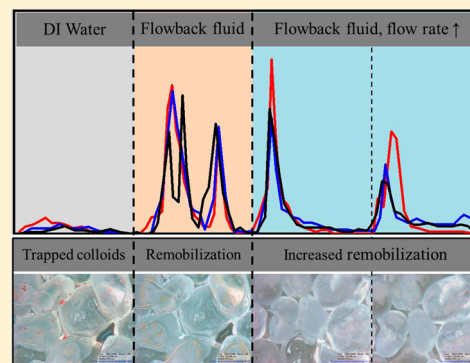
^{||}Department of Plant, Soil and Microbial Sciences, Environmental Science and Policy Program, Michigan State University, East Lansing, Michigan 48824, United States

[⊥]SIMBIOS Centre, University of Abertay Dundee, Bell Street, Dundee, DD1 1HG, Scotland

[#]Department of Agricultural and Biological Engineering, University of Florida, Gainesville, Florida 32611, United States

Supporting Information

ABSTRACT: Hydraulic fracturing is expanding rapidly in the US to meet increasing energy demand and requires high volumes of hydrofracking fluid to displace natural gas from shale. Accidental spills and deliberate land application of hydrofracking fluids, which return to the surface during hydrofracking, are common causes of environmental contamination. Since the chemistry of hydrofracking fluids favors transport of colloids and mineral particles through rock cracks, it may also facilitate transport of in situ colloids and associated pollutants in unsaturated soils. We investigated this by subsequently injecting deionized water and flowback fluid at increasing flow rates into unsaturated sand columns containing colloids. Colloid retention and mobilization was measured in the column effluent and visualized in situ with bright field microscopy. While <5% of initial colloids were released by flushing with deionized water, 32–36% were released by flushing with flowback fluid in two distinct breakthrough peaks. These peaks resulted from 1) surface tension reduction and steric repulsion and 2) slow kinetic disaggregation of colloid flocs. Increasing the flow rate of the flowback fluid mobilized an additional 36% of colloids, due to the expansion of water filled pore space. This study suggests that hydrofracking fluid may also indirectly contaminate groundwater by remobilizing existing colloidal pollutants.



INTRODUCTION

Natural gas extraction from deep shale gas deposits such as the Marcellus Shale in the Northeastern United States has become a rapidly expanding and controversial fossil fuel recovery practice to achieve energy independence.¹ High-pressure hydraulic fracturing (“hydrofracking”) techniques have been extensively used in the drilling process and typically require an injection of 8–40 million liters of hydrofracking fluid into wellbores in order to increase the permeability of deep rock strata where gas and oil are trapped. Compared to conventional gas drilling, there is considerable environmental concern and debate over the practice of hydrofracking and its waste management.^{2–5}

In the hydrofracking process, approximately 10–40% of the injected fracking fluids surge back to the surface within a two-week period as flowback fluid.^{6,7} Although specific details regarding the concentration and chemical composition of the hydrofracking fluid is most often concealed for proprietary

purposes (www.fracfocus.org), typical components include water, lubricants, organic solvent and polymers (e.g., alcohols, organic acids), biocides, and sand particles.⁸ In addition to the chemicals in the original hydrofracking fluid, the flowback fluids have been reported to contain substances extracted from the fracked rock formations, including natural organic matter, heavy metals, and radionuclides.^{1,9,10} Land application of flowback fluids as a means of waste disposal has been permitted by several states in the US, though many regulations are currently under review because of potential impacts of this practice on the environment, such as severe vegetation damage and mortality.⁵ While there is evidence linking groundwater contamination to various hydrofracking processes,^{6,7} little is

Received: March 25, 2014

Revised: June 4, 2014

Accepted: June 6, 2014

Published: June 6, 2014

known about the effects of deliberate disposal or accidental spills of hydrofracking fluids on colloid mobilization in partially water saturated soils (the unsaturated zone) and on groundwater contamination. Suspended colloids in subsurface water (e.g. mineral fragments, clays, and organic particulates) have been implicated in the transport of colloid-associated contaminants (e.g., heavy metals and radionuclides) that result in soil and groundwater contamination.^{11–13} Depending on soil texture and composition, colloid mobilization may also promote clogging and related reductions in soil permeability.¹⁴ Moreover, extensive research has indicated that colloid mobilization in soils is strongly dependent on key chemical constituents known to make up the hydrofracking fluids, including inorganic salts (e.g., Na^+ , Ca^{2+} , Cl^-) and organic compounds (e.g., surfactants and humic substances).^{12,15}

According to the Derjaguin–Landau–Verwey–Overbeek (DLVO) theory, the primary reason that colloids are mobile in a porous medium is because they are electrostatically repelled from each other and from grain surfaces. While the presence of electrolytes, measured as ionic strength, screens and/or neutralizes this surface charge and thus reduces electrostatic repulsion and hinders colloid mobility,^{15,16} some organic compounds (e.g., anionic surfactants, humic substances) may have the opposite effect. When these organic compounds adsorb onto colloid and grain surfaces they increase the magnitude of their negative surface charge, thereby causing electrostatic repulsion between colloids and the porous medium, which reduces aggregation and enhances colloid mobilization.^{17,18} In some cases, this is facilitated by the fact that organic macromolecules also form hairy structures on the colloid surface and/or the solid–water interface that establishes steric repulsion.^{19,20} Like organic compounds, surfactants affect colloid movement by making them more mobile. Surfactants may contribute to colloid decementation by extending the electrokinetic shear plane when adsorbed surfactants are orientated with hydrophobic tails away from the surface,²¹ making the surfaces more hydrophobic, or increasing unsaturated water flow and facilitating solute transport;^{22–24} thus resulting in increased colloid transport.^{25–27} Also, reduced surface tension caused by surfactant addition is known to affect colloid interactions with interfaces found in unsaturated porous media. In particular, colloid pinning at the air–water–solid (AWS) interface or contact line have been reported to be reduced because of weakened capillary forces.^{18,28,29} Given these effects of key components of the fracking fluid on colloid mobilization processes, accidental or deliberate land application of flowback fluid may profoundly alter colloid mobilization and subsequent transport of other colloid-associated contaminants in soil and groundwater.

Our objective was to determine emerging trends of hydrofracking fluid effects on colloid transport processes. We hypothesized that flowback fluid mobilizes colloids in soil and tested this by visualizing and quantifying colloid transport as affected by flowback fluid in unsaturated sand. Briefly, sand columns with known quantities of deposited colloids were flushed with deionized water (DI “Stage 1”), followed by flushing events with flowback fluid at increasing flow rates (“Stage 2–4”). Colloid release was quantified from effluent concentration measurements throughout the flushing sequences. Simultaneous in situ visualization of colloid behavior was done with bright field microscopy to help elucidate colloid mobilization mechanisms at the pore-scale.

■ MATERIALS AND METHODS

Flowback Fluid. The flowback fluid used in this study originated from a vertical gas well in the Marcellus Shale of central New York State, USA, that was fracked in October 2010. It was filtered through a $0.45\ \mu\text{m}$ membrane before use and analyzed for the following: metal identification and concentration, chloride concentration, total organic carbon, pH, electrical conductivity, surface tension, and radioactivity (Supporting Information S1).

Colloids and Porous Media. Red carboxylated polystyrene microspheres of $3.0\ \mu\text{m}$ were used in the experiments (Polysciences, Inc., Warrington, PA, USA). These colloids were washed with DI water, filtered at $0.45\text{-}\mu\text{m}$ membrane, and resuspended in a CaCl_2 solution of 10 mM ionic strength (IS) to form working suspensions of $626 \pm 78\ \text{mg/L}$. The pH of the CaCl_2 solution was adjusted with 1 M NaOH solution to match the pH of DI water (5.9), and the pH of flowback fluid was 6.9. In order to emulate the effects of real flowback fluid on colloid transport behavior, the pH of flowback fluid was not adjusted. The choice for using model environmental colloids was based on their well-known physical and chemical properties, which were necessary to elucidate the transport processes taking place when exposed to chemically complex flowback fluid. The stabilities of colloid suspensions in DI water, CaCl_2 solution of 10 mM IS, and flowback fluids were determined by measuring the change of colloid hydrodynamic diameter (D_h) over time using a zetasizer (Zetasizer Nano ZS, Malvern, Worcestershire, UK), as described in Supporting Information S7. The porous media used consisted of angular translucent quartz sand (Size 2#, AGSCO Corporation, Hasbrouck Heights, NJ, USA) that was sieved to 0.59–0.84 mm and cleaned to remove surface impurities by the “HCl/heat” method.³⁰ Electrophoretic mobility (EM) of the colloids and sand fragments (Supporting Information S6) suspended in DI water, the CaCl_2 solution, and flowback fluid was measured using the above zetasizer, and zeta potentials were calculated from the EM data by Smoluchowski’s equation.

Colloid Mobilization Experiments. The colloid mobilization experimental setup is illustrated in Figure S1. A $1 \times 1 \times 20\ \text{cm}$ glass column was wet-packed in DI water with a fixed amount of sand, resulting in a porosity of $0.40\ \text{cm}^3/\text{cm}^3$. The column was capped with a porous ceramic suction plate of 40–50 μm pore size at both ends. The column was maintained in unsaturated conditions by connecting a hanging water column at the outlet (capillary pressure of $-2.5\ \text{kPa}$) and a micropurge peristaltic pump at the inlet at a constant flow rate of 0.3 mL/min. At the start of each experiment, a 1 mL pulse of the colloid working suspension (10 mM IS by CaCl_2 solution) was introduced at the same flow rate, followed by four 25 mL flushing stages: 1) DI water, 0.3 mL/min; 2) flowback fluid, 0.3 mL/min; 3) flowback fluid, 1.5 mL/min; 4) flowback fluid, 3.0 mL/min. The initial injection of 1 mL CaCl_2 solution at 10 mM IS was used to ensure strong colloid retention in the porous medium at the beginning deposition phase, and the retained colloids were then subject to the above four flushing stages.

To allow for destructive measurements of the distribution of retained colloids in the sand column after each stage, three experiments (A, B, and C) were performed, with three replicates each. Experiment A consisted of Stage 1, Experiment B consisted of Stage 1 and 2, and Experiment C included all four stages. During the experiments, effluent samples were collected in cuvettes at 4 min intervals, and their volume

recorded. Colloid concentration was measured with light absorbance using a spectrophotometer (Spectronic 501, Milton Roy, Ivyland, PA, USA) at a wavelength of 550 nm, with Figure S2 showing the linear calibration curve ($R^2 = 0.996$). Given that flowback fluid and DI water have different absorbances (0.026 vs 0.000, respectively), additional colloid-free experiments of Stages 1 and 2 were conducted to determine the changes in background light absorbance due to pore-water exchange from DI to flowback fluid. This information was then used to correct by subtraction the spectrophotometric readings of effluent samples in experiments with colloids. To monitor the elution of the flowback fluid (as pore-water was switched from DI to flowback fluid), effluent samples from Experiment B were also analyzed for chloride concentration by ion chromatography. During the experiments, pore-scale colloid retention and mobilization processes were visualized in situ with a horizontally mounted digital bright field microscope (KH-7700, Hirox-USA, River Edge, NJ, USA), following Morales et al.³¹ and Zhang et al.³² Random pores located between 1 and 3 cm from the top of the column were selected for observation and still images or videos captured throughout the experiment. Finally, the depth distribution of retained colloids was determined following a previously established protocol.^{33,34} Briefly, the sand was carefully excavated from the column and divided into ten 2 cm segments. The sand in each segment was then immersed in 5 mL of DI water in order to release the deposited colloids from the sand. The colloid concentration was then measured in the supernatant. The retained colloid mass per unit mass was calculated and reported as a function of column depth.

Details on how sand moisture contents were determined and on the statistical analyses performed can be found in Supporting Information S5 and S8.

RESULTS

Characteristics of Hydrofracking Flowback Fluid. The hydrofracking flowback fluid was rich in Ca and Na (300 and 493 mg/L, respectively) and had a high chloride concentration (1897 mg/L, Table 1), similar to other flowback fluids in the Northeastern US.^{8,9} The near-neutral pH value of 6.9 indicates that either the flowback fluid contained no acid additives or the acids were effectively neutralized by the strata at the

Table 1. Flowback Fluid Characteristics^a

parameter	value			
metal concn (mg/L)	<i>Ba</i>	5.3 ± 0.0	<i>Na</i>	493 ± 4
	<i>Ca</i>	300 ± 5	<i>S</i>	176 ± 2
	<i>K</i>	77 ± 1	<i>Sr</i>	22 ± 0
	<i>Mg</i>	34 ± 0		
	chloride concn (mg/L)	1897 ± 7		
ionic strength (mM) ^b	68			
pH	6.9 ± 0.0			
electrical conductivity (mS/cm)	6.1 ± 0.0			
TOC (mg/L) ^c	1593 ± 78			
surface tension (mN/m)	35.1 ± 0.1			
Pb-214	below detection limit			

^aValues are averages over the sample replicates of the different analyses ($n = 4$ for TOC, $n = 3$ for all others) ± one s.d.; all samples were filtered through a 0.45- μ m membrane before analysis.

^bCalculated from the mean concentrations of chloride and metals.

^cTotal organic carbon.

hydrofracking site. The high TOC value (1593 mg/L) suggests that a great amount of organic compounds were present, including organic additives in the original hydrofracking fluids, as well as extracted natural organic matter from the shale formation.^{8,9,35} Finally, the low surface tension of 35.1 mN/m indicates the presence of amphiphilic compounds (i.e., surfactants) in the flowback fluid, while the absence of radioactivity (as indicated by the nondetect of Pb-214) illustrates the short contact time between the fracking or flowback fluids and the shale formation.

Two-way ANOVA analyses of EM and ζ -potential indicated that there was a significant interaction between percolation liquid and particle type ($p < 0.0001$ in both cases), with negative EM and ζ -potential values for colloids suspended in DI water or CaCl₂ solution, and significantly higher and positive values when suspended in flowback fluid. This was likely a result from charge reversal due to either specific adsorption of cations (e.g., Ca²⁺ and Mg²⁺) on or accumulation of counterions (e.g., Ca²⁺ and Mg²⁺) near the colloid and sand surface.^{36–38}

Colloid Effluent Breakthrough Curves. The colloid breakthrough concentrations of Experiments A (Stage 1), B (Stages 1–2), and C (Stages 1–4) are shown in Figure 1. During the flush event with DI water, <5% of the injected

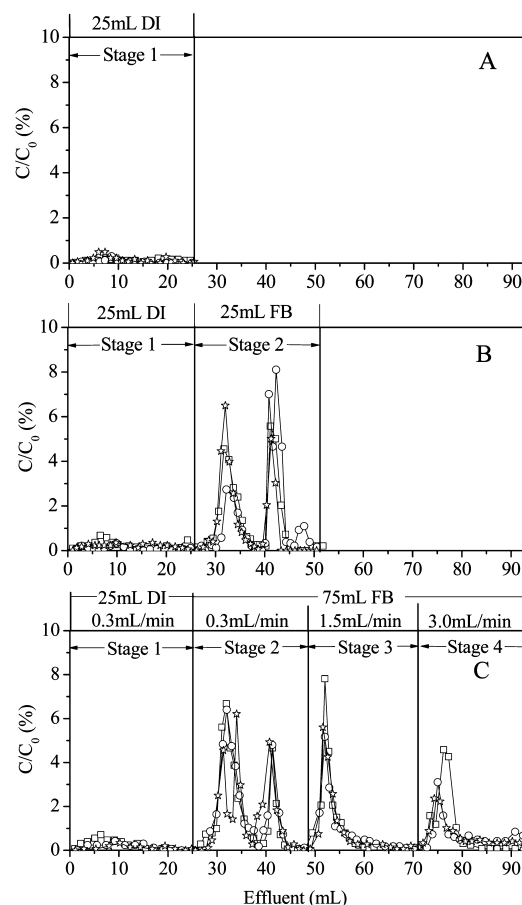


Figure 1. Effluent breakthrough curves in columns containing previously deposited colloids in 10 mM IS by CaCl₂ solution. Flush events mobilized colloids with A) DI water, B) DI and flowback fluid (FB), and C) DI and transient FB, showing the three replicates per treatment. Vertical lines indicate the approximate moment when the influent liquid at each stage reached the bottom of the column.

Table 2. Flow Rates, Volumetric Water Content, and Percentages of Colloids Recovered in Effluent for Experiments A, B, and C after Stages 1, 2, 3, and 4 (First Four Lines)^{a,g}

stage	influent ^b	flow rate (mL/min)	moisture content (cm ³ /cm ³) ^c	colloid recovery (%)		
				Experiment A	Experiment B	Experiment C
1	DI	0.3	0.180 ± 0.013 (a)	2 ± 1 (e)	5 ± 2 (e)	4 ± 1 (e)
2	FB	0.3	0.176 ± 0.014 (a)		32 ± 3 (c)	36 ± 1 (c)
3	FB	1.5	0.224 ± 0.003 (b)			19 ± 1 (d)
4	FB	3.0	0.257 ± 0.007 (c)			17 ± 1 (d)
recovery from sand (%) ^d				87 ± 2 (a)	57 ± 6 (b)	21 ± 3 (d)
total recovery (%) ^e				89 ± 1 (f)	94 ± 6 (f)	98 ± 1 (f)
not recovered (%) ^f				11 ± 1 (f)	6 ± 6 (f)	2 ± 1 (f)

^aAll percentages are given as the amount of colloids added to the column. ^bDI is DI water; FB is flowback fluid. ^cMoisture content was determined at the end of each run as well as between Stages 2, 3, and 4. ^dPercentage of colloids recovered after washing the sand at the end of the Experiments A, B, and C. ^eSum of colloids recovered in effluent and from sand washing. ^fColloids not accounted for and/or firmly attached to the sand particles. Observed values are means ± 1 standard deviation ($n = 6$ for Stage 2 moisture content, $n = 3$ for all other values). Different letters between parentheses indicate that the values are significantly different at $p < 0.05$. ^gThe last 3 lines indicate for each of the experiments, the colloids recovered after washing with water, total amount of colloids in effluent and wash water, while the last line indicates the % of colloids not accounted.

colloids (Table 2) were recovered in the effluent (Stage 1 in Figure 1A–C). The addition of the flowback fluid at 0.3 mL/min produced two distinct colloid breakthrough peaks (Stage 2 in Figure 1B–C), in which 32–36% of the injected colloids were remobilized from the sand column. The onset of the first peak was associated with an increase in chloride concentration (Figure 2), indicating the displacement of the pore water with

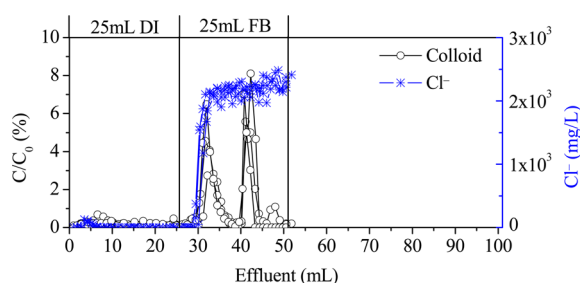


Figure 2. Superimposed colloid and chloride concentration in the effluent of Experiment B. Colloid concentration corresponds to colloid mobilization of a column containing previously deposited colloids in 10 mL by CaCl₂ solution that was flushed with deionized water (DI), followed by a flush of flowback fluid (FB).

the flowback fluid. This is evident from concurrence of the apex of the first flowback fluid induced peak with the plateau of effluent chloride concentrations asymptotically approaching that of the original flowback fluid (Figure 2, Table 1). The onset of the second peak occurred after the sand was fully immersed in the flowback fluid. The increase in the flow rate from 0.3 to 1.5 mL/min and 1.5 to 3.0 mL/min each caused another peak of colloid release from the column (19% and 17% of the applied colloids, respectively, Table 2), as illustrated in Stages 3 and 4 in Figure 1C. Unlike the first flush event with the flowback fluid (Stage 2 in Figure 1B–C), no double colloid release peaks were observed when the flow rate of the flowback fluid was increased. This indicates that only the chemical perturbation of switching pore water from DI water to the flowback fluid is responsible for the unusual double peaks.

Distribution of Colloids with Depth. In all three experiments (A, B, C), the majority of colloids that remained in the sand after flushing with DI and/or flowback fluid were recovered by washing after the experiment. The washing procedure recovered 87%, 57%, and 21% of the initial applied

amount of colloids for Experiments A, B, and C, respectively (Table 2). Figure 3 shows the depth distribution of the colloids

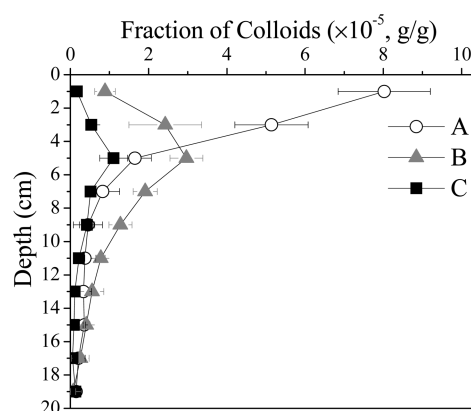


Figure 3. Depth distribution of colloids remaining in the column after Experiments A–C, in which the fraction of colloids is expressed on a weight basis per gram of sand.

remaining in the sand column, with results from statistical analysis given in Table S1. There was a significant interaction between treatment and depth ($p < 0.0001$), indicating that the depth distribution of colloids retained in the sand column was different for the different experimental treatments. For DI experiment A, the amount of colloids retained in the sand column significantly decreased with depth, following a slightly hyperexponential profile, as the colloid concentration close to the column inlet was greater than what is expected from an exponential distribution. Flowback fluid Experiments B and C showed similar depth profiles of retained colloids, with both a significant peak at 4–6 cm depth, but with a significantly smaller amount of colloids retained after Experiment C than after Experiment B (Figure 3, Table S1). This type of profile shape has also been observed previously for carboxylated polystyrene microspheres,³⁹ bacteria,⁴⁰ viruses,⁴¹ and protozoa,⁴² attributed to processes of straining, attachment/detachment, and surface heterogeneity.

Despite the considerable amount of colloids recovered by washing the sand after the experiments, between 2 and 11% of applied colloids were unaccounted for in the colloid mass balance summarized in Table 2. It is interesting to note that the percentage of colloids accounted for increased with the amount

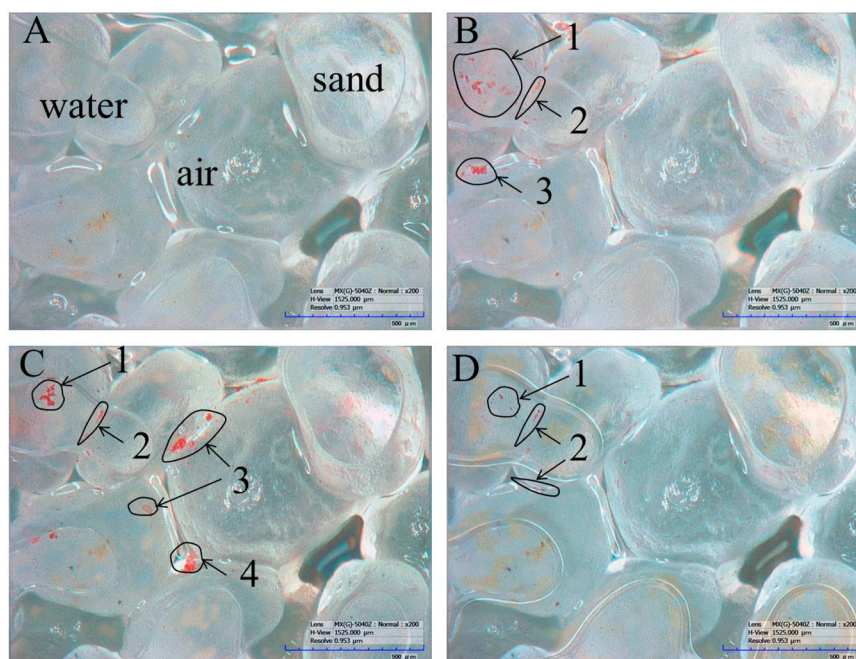


Figure 4. Bright field microscope images of colloids retained in the unsaturated sand in Experiment B (one replicate run shown) at A) start, and after B) colloids are injected, C) end of Stage 1 (25 mL DI water), D) end of Stage 2 (25 mL flowback fluid). Retention sites: 1—solid–water-interface (SWI), 2—grain–grain contact, 3—air–water–solid (AWS) interface, 4—air–water-interface (AWI).

and flow rate of the flowback fluid applied, e.g. it was the smallest for Experiment A (89%) and greatest for C (98%). Although the increase is not significant ($p = 0.14$), this trend is supported by images collected by bright field microscopy, showing most colloid aggregates remaining on the grain surface after washing for the DI-only Experiment A and the least after the high flow rate flowback fluid Experiment C (Figure S3).

In Situ Visualization of Colloid Movement. The visualization of real time pore-scale processes with bright field microscopy provided valuable information for the mechanistic understanding of colloid retention and mobilization at the column inlet where most colloids were retained. As shown in Figure 4B–D, colloids were primarily retained at the solid–water interface (SWI, site 1) and at the air–water–solid interface (AWS, site 3); while a small amount was retained at the grain–grain contacts (site 2). During the flush event in Stage 1 (DI water at 0.3 mL/min), both the attached and suspended colloids remained in the form of large aggregates (Figure 4B–C, Video S1). While slight colloid aggregation occurred in flowback fluid (Figure S5), all stabilized aggregate sizes were smaller than $5.6 \mu\text{m}$ during 60 min stability tests, and colloid suspensions in static batch phase were relatively stable with the average D_h of $3.13 \pm 0.34 \mu\text{m}$ in DI water, $3.13 \pm 0.27 \mu\text{m}$ in CaCl_2 solution of 10 mM IS, and $3.73 \pm 0.85 \mu\text{m}$ in flowback fluid, respectively (Supporting Information S7). Nonetheless, colloid aggregation is expected to be greatly enhanced under the influence of flow field, due to flow-induced and orthokinetic aggregation.^{40,43,44} Therefore, colloid flocs much greater than $5.6 \mu\text{m}$ were readily observed, and the disaggregation of these large colloid flocs into small colloid aggregates, as induced by steric repulsion from flowback fluid, may elicit the unique colloid transport behavior observed here. The larger colloid aggregates cannot easily migrate through soil pore space even after becoming detached from the retention sites due to size restrictions. Therefore, large aggregates remain retained by straining and interstitial filtration.^{33,45} Smaller

aggregates and individual colloids were apparently weakly captured at the AWS interface (Video S1) where they oscillated slowly. This behavior is likely due to the low velocity in this water restricted region.³² However, when the influent was switched to the flowback fluid, the majority of the weakly retained colloids were released, and only a minor portion of those visible at the monitored pore remained retained in the column throughout the flushing event (Figure 4D). Video S1 illustrates this re-entrainment phenomenon. At time 1:26 min into this video, colloids retained at the SWI became detached, and at 2:22 min colloid aggregates at the AWS interface became disaggregated and re-entrained to the bulk flowing water. The direct visualization demonstrated the important role of colloid aggregation and disaggregation in colloid mobilization, which is discussed in detail in the following section.

DISCUSSION

Colloid Retention and Mobilization As Affected by DI Water. In order to better understand the colloid retention and mobilization mechanisms, we will first compare the results of experiment A (DI flush) and experiment B and C (flowback fluid flush). Interestingly, the observed minimal colloid mobilization (<5%) during the DI water flush of experiment A (Figure 4, Video S1) does not follow the behavior predicted by classic DLVO theory. For the 10 mM IS CaCl_2 solution in which the colloids were injected into the sand column, we expect a large amount of colloids to be retained in the porous media initially. Moreover, DLVO calculations (Supporting Information S6, Table S3, Figure S4) indicate that the colloids would aggregate and deposit onto the sand grain surface at the secondary energy minimum, as suggested by others.^{46,47} According to classic DLVO theory, upon switching the flow from the CaCl_2 solution to DI water, the secondary energy minimum should be eliminated (Table S3, Figure S4), thereby releasing deposited colloids from the sand. This theory agrees with observations made by others in cases where monovalent

electrolytes (NaCl or KCl) were involved.^{39,47–51} However, in the presence of divalent electrolytes such as Ca^{2+} used in the present study, colloid mobilization is found to be minimal when switching from the CaCl_2 solution to DI water or a KCl solution of lower IS.^{47,52} This suggests that cation bridging by Ca^{2+} ^{52–54} was responsible for the colloid aggregation and deposition that occurred in Experiment A (DI water). Colloid aggregation also contributed to the straining process, which was corroborated by the visual observation (Figure 4, Video S1) and the hyperexponential profile of colloid distribution with depth (Figure 3). The hyperexponential profile has been frequently observed and attributed to colloid straining,⁴⁵ retention in low velocity regions,⁵⁵ or colloid population heterogeneity.⁵⁶ In this study, retention of colloid aggregates by straining and low velocity regions were likely responsible for the deposition profile.

Effect of Flowback Fluid on Colloid Retention and Mobilization. Upon switching to the flowback fluid in Stage 2, Experiment B, the colloids were remobilized (Figure 1 and Table 2). While there was only 2% colloid effluent recovery in experiment A, a total of 37% was recovered in the effluent in experiment B. Both the breakthrough curves and the visualization (Figure 4 and Video S1, respectively) indicate that the flowback fluid has a high potential to mobilize the colloids. Like in the case of DI-water, this observation disagrees with DLVO calculations (Table S3, Figure S4). In these energy profiles, favorable conditions for aggregation and deposition are predicted for colloids in the flowback fluid due to the absence of the primary energy barrier. Colloid remobilization in Stage 2 was probably a result from the coupled effect of steric repulsion and cation exchange caused by the flushing of flowback fluid. Steric repulsion is expected to result from the sorption of dissolved organic matter and surfactants in the flowback fluid onto colloid and sand surfaces that promote colloid disaggregation and detachment.^{18,20,57} Cation exchange of residual Ca^{2+} from the colloid deposition stage is expected to occur with monovalent cations⁵⁸ (e.g., Na^+) from the flowback fluid that break down calcium bridges between colloids and sand surfaces and subsequently promote their release.

Colloid remobilization during washing was probably facilitated by the incomplete release of adsorbed Ca^{2+} between the colloid and the substrate during the flowback fluid flushing stages for Experiments B–C with “flowback fluid flush”. We suspect that release of adsorbed Ca^{2+} was allowed to go to completion when column sections previously exposed to flowback fluid were submerged in DI water during sand washing. As a result, calcium bridges were likely broken and the colloids subsequently released. In contrast, sand washing of Experiment A with “DI flush” resulted in appreciable colloid release despite the lack of monovalent cations in the DI available for exchange and breaking of Ca^{2+} bridges (Table 2 and Figure S3).

It has not escaped our notice that different concentrations of monovalent cations in the flowback fluid would have probably resulted in a different degree of colloid release and stress the importance of exploring this variable in follow-up studies. The increased colloid mobilization by the flowback fluid may additionally be caused by the reduction of the fluid surface tension that can lead to flow field perturbations^{22,59} and reduced retention at the AWS interface.^{28,29}

An interesting observation is that double peaks of colloid release are associated with the switch of DI water to flowback fluid (Figure 1B–C). The first peak concurred with the arrival

of the flowback fluid, which could be attributed to the processes discussed above: flow perturbation, reduced colloid retention at the AWS interface, and increased steric repulsion. To facilitate the increased flux, larger pores are filled and capillary pressure is decreased, resulting in a greater meniscus radius. This results in Haines jumps filling up the pore in less than a second (see Video S1 at 3:42 min) causing high drag forces that can detach colloids from sand grains. Haines jumps were first proposed by Haines in 1930⁶⁰ to refer to a sudden drop in capillary pressure when the nonwetting phase (e.g., air) passes from a pore neck into a wider pore body displacing the wetting phase (e.g., water) and vice versa. Also, the large meniscus radii would decrease the capillary force responsible for colloid retention at the AWS interface^{28,29} and subsequently facilitate the colloid release from the AWS interface. The steric repulsion by adsorption of organic compounds such as humic substances could be also responsible for colloid mobilization. However, its effect on the disaggregation of colloids may have an initial lag time because the disaggregation of colloid aggregates is a slow kinetic process.^{57,61} We hypothesize that this slow disaggregation of the large colloid aggregates caused the second colloid release peak as the smaller colloid aggregates could pass through the narrow neck of the soil pore space.

Although concrete explanations for the processes causing the second peak require additional research, the microscope images indicate that colloid disaggregation takes place during the elution of this peak as a slower kinetic process. For instance, at 2:22 min in Video S1, colloid disaggregation occurred more than a minute after the arrival of the flowback fluid. Yet, the time gap between the two peaks (~30 min, Figure 2) was much longer than a minute, either indicating that other (unobserved) parts of the column had an even slower response or that colloids disaggregated in the top of the column were delayed in smaller pores further down.

Effect of Increasing Flux on Colloid Mobilization. Finally, while two peaks were observed after first switching from DI water to flowback fluid, only a single peak was observed for effluent breakthrough of Experiment C as a result of the increase in flow rate of the flowback fluid (Figure 1C). This increase in remobilization can be explained by the hydrodynamic torque exerted on colloids, which was sufficiently strong to induce detachment.^{39,62,63} High flow rates also decrease the volume of low-flow or stagnant zone regions where colloids can be immobilized,^{39,62,63} thereby increasing the opportunity for mobilization. An additional element responsible for the increased mobilization can be attributed to the significant increase in moisture content of the porous medium during heightened flow rate flushing ($p < 0.0001$, Table 2). At greater flow velocity (at 3:30 min in Video S1), pore water content increased and capillary pressure decreased. As a result, pore spaces suddenly filled up (see 3:42 min for example). This caused both high local water velocities and flow reversals, which dislodged strained colloids⁶⁴ by eliminating AWS interface retention sites. In addition, larger pores with larger throat sizes became available for displaced strained colloids to move through.²⁵

ENVIRONMENTAL IMPLICATIONS

By showing that flowback fracking fluid can remove colloids from sand grains and wash them out of unsaturated sand, our results suggest that land application of flowback fluids (whether accidental or deliberate) can contaminate groundwater resources through either the intrinsic chemical constituents of

the flowback fluid or mobilization of colloid-associated soil contaminants. This indicates that infiltration of flowback fluid could turn soils into an additional source of groundwater contaminants such as heavy metals, radionuclides, and microbial pathogens. Spills occurring near roadside ditches and agricultural fields can therefore potentially mobilize oils and agrochemicals to surface- and ground-waters. While this study was performed in model systems using polystyrene microspheres and quartz sand, the observed colloid mobilization mechanisms should be general and provide initial insights to further investigations involving more complex and heterogeneous soil environments. The actual extent of soil colloid mobilization by flowback fluid at a given site will not only be affected by flow rate (Figure 1, Figure 3) but also be highly dependent on factors like soil texture, structure, and composition at the site, as well as flowback fluid characteristics. Future work will test the reported mobilization trends in structured and clayey (field) soils, with particular care for permeability reduction below zones of *in situ* soil colloid mobilization. In order to thoroughly evaluate whether gas drilling by hydrofracking is a safe energy source, it is imperative to include waste disposal and accidental spills in its environmental impact assessment. Likewise, it is essential to know how fracking fluid affects the environment in case there is a spill, as this process knowledge is required to design effective ways to mitigate environmental accidents. Ultimately, environmentally sound exploration of shale gas resources requires safe and effective management of the hydrofracking flowback fluid to ensure protection of groundwater and surface water resources.

■ ASSOCIATED CONTENT

Supporting Information

S1. Chemical analysis of flowback fluid; S2. Experimental setup; S3. Colloid calibration curve; S4. Column dissection experiments; S5. Assessment of sand moisture contents; S6. Interaction energy calculation; S7. Colloid stability and electrophoretic mobility; S8. Statistical analyses; Video S1. This material is available free of charge via the Internet at <http://pubs.acs.org>.

■ AUTHOR INFORMATION

Corresponding Author

*Phone: 607 255 2489. E-mail: tss1@cornell.edu. Corresponding author address: 206 Riley Robb Hall, Cornell University, Ithaca, NY 14853, United States.

Notes

The authors declare no competing financial interest.

■ ACKNOWLEDGMENTS

We thank Steven Pacenka for assistance, Douglas Caveney for help with constructing the flow chambers, and Shree Giri for help with chemical analysis. This work was supported by the Chinese Scholarship Council (W.S.), National Natural Science Foundation of China (Project #41301534), Hatch Federal Formula Funds (Project #2010-11-257) awarded via Cornell University's College of Agriculture & Life Sciences, USDA-NIFA Hatch Program (MICL02248), and the National Science Foundation (Project #0635954). V.L.M. was supported by a Marie Curie Action International Incoming Fellowship (FP7-PEOPLE-2012-SoilArchnAg). The views expressed in this paper are those of the authors alone and do not necessarily

reflect the views of the authors' organizations or the funding agencies.

■ REFERENCES

- (1) Kargbo, D. M.; Wilhelm, R. G.; Campbell, D. J. Natural gas plays in the Marcellus Shale: Challenges and potential opportunities. *Environ. Sci. Technol.* **2010**, *44* (15), 5679–5684.
- (2) Jackson, R. B.; Vengosh, A.; Darrah, T. H.; Warner, N. R.; Down, A.; Poreda, R. J.; Osborn, S. G.; Zhao, K.; Karr, J. D. Increased stray gas abundance in a subset of drinking water wells near Marcellus shale gas extraction. *Proc. Natl. Acad. Sci. U. S. A.* **2013**, *110* (28), 11250–11255.
- (3) Bamberger, M.; Oswald, R. E. Impacts of gas drilling on human and animal health. *New Solutions* **2012**, *22* (1), 51–77.
- (4) Davies, R. J. Methane contamination of drinking water caused by hydraulic fracturing remains unproven. *Proc. Natl. Acad. Sci. U. S. A.* **2011**, *108* (43), E871–E871.
- (5) Adams, M. B. Land application of hydrofracturing fluids damages a deciduous forest stand in west virginia. *J. Environ. Qual.* **2011**, *40* (4), 1340–1344.
- (6) Arthur, J. D.; Bohm, B.; Layne, M. In *Ground Water Protection Council 2008 Annual Forum*; Cincinnati, OH, 2008.
- (7) Wood, R.; Gilbert, P.; Sharmina, M.; Anderson, K.; Footitt, A.; Glynn, S.; Nicholls, F. Shale gas: a provisional assessment of climate change and environmental impacts; The Tyndall Centre, University of Manchester, 2011.
- (8) NYDEC Chapter 5 Natural gas development activities & high-volume hydraulic fracturing, New York State Department of Environmental Conservation, 2011.
- (9) Wolford, R. *Characterization of organics in the Marcellus shale flowback and produced waters*. M.S. Dissertation, The Pennsylvania State University, University Park, PA, 2011.
- (10) Haluszczak, L. O.; Rose, A. W.; Kump, L. R. Geochemical evaluation of flowback brine from Marcellus gas wells in Pennsylvania, USA. *Appl. Geochem.* **2013**, *28*, 55–61.
- (11) McCarthy, J. F.; Zachara, J. M. Subsurface transport of contaminants. *Environ. Sci. Technol.* **1989**, *23* (5), 496–502.
- (12) McDowell-Boyer, L. M.; Hunt, J. R.; Sitar, N. Particle transport through porous media. *Water Resour. Res.* **1986**, *22* (13), 1901–1921.
- (13) Warner, N. R.; Christie, C. A.; Jackson, R. B.; Vengosh, A. Impacts of shale gas wastewater disposal on water quality in western Pennsylvania. *Environ. Sci. Technol.* **2013**, *47* (20), 11849–11857.
- (14) Goldenberg, L. C.; Magaritz, M.; Mandel, S. Experimental investigation on irreversible changes of hydraulic conductivity on the seawater-freshwater interface in coastal aquifers. *Water Resour. Res.* **1983**, *19* (1), 77–85.
- (15) Ryan, J. N.; Elimelech, M. Colloid mobilization and transport in groundwater. *Colloids Surf, A* **1996**, *107* (0), 1–56.
- (16) Bradford, S. A.; Torkzaban, S. Colloid transport and retention in unsaturated porous media: A review of interface, collector-, and pore-scale processes and models. *Vadose Zone J.* **2008**, *7* (2), 667–681.
- (17) Iglesias, G. R.; Wachter, W.; Ahualli, S.; Glatter, O. Interactions between large colloids and surfactants. *Soft Matter* **2011**, *7* (10), 4619–4622.
- (18) Zhuang, J.; Goepfert, N.; Tu, C.; McCarthy, J.; Perfect, E.; McKay, L. Colloid transport with wetting fronts: Interactive effects of solution surface tension and ionic strength. *Water Res.* **2010**, *44* (4), 1270–1278.
- (19) Morales, V. L.; Zhang, W.; Gao, B.; Lion, L. W.; Bisogni, J. J., Jr.; McDonough, B. A.; Steenhuis, T. S. Impact of dissolved organic matter on colloid transport in the vadose zone: deterministic approximation of transport deposition coefficients from polymeric coating characteristics. *Water Res.* **2011**, *45* (4), 1691–1701.
- (20) Phenrat, T.; Song, J. E.; Cisneros, C. M.; Schoenfelder, D. P.; Tilton, R. D.; Lowry, G. V. Estimating attachment of nano- and submicrometer-particles coated with organic macromolecules in porous media: Development of an empirical model. *Environ. Sci. Technol.* **2010**, *44* (12), 4531–4538.

- (21) Clayfield, E. J.; Smith, A. L. Adhesion and detachment of solid colloidal particles in aqueous ionogenic surfactant media. *Environ. Sci. Technol.* **1970**, *4* (5), 413–416.
- (22) Henry, E. J.; Smith, J. E.; Warrick, A. W. Solubility effects on surfactant-induced unsaturated flow through porous media. *J. Hydrol.* **1999**, *223* (3–4), 164–174.
- (23) Henry, E. J.; Smith, J. E.; Warrick, A. W. Surfactant effects on unsaturated flow in porous media with hysteresis: horizontal column experiments and numerical modeling. *J. Hydrol.* **2001**, *245* (1–4), 73–88.
- (24) Henry, E. J.; Smith, J. E. The effect of surface-active solutes on water flow and contaminant transport in variably saturated porous media with capillary fringe effects. *J. Contam. Hydrol.* **2002**, *56* (3–4), 247–270.
- (25) Saiers, J. E.; Lenhart, J. J. Colloid mobilization and transport within unsaturated porous media under transient-flow conditions. *Water Resour. Res.* **2003**, *39* (1).
- (26) Ryan, J. N.; Gschwend, P. M. Effect of solution chemistry on clay colloid release from an iron oxide-coated aquifer sand. *Environ. Sci. Technol.* **1994**, *28* (9), 1717–1726.
- (27) Shang, J. Y.; Flury, M.; Chen, G.; Zhuang, J. Impact of flow rate, water content, and capillary forces on in situ colloid mobilization during infiltration in unsaturated sediments. *Water Resour. Res.* **2008**, *44* (6).
- (28) Gao, B.; Steenhuis, T. S.; Zevi, Y.; Morales, V. L.; Nieber, J. L.; Richards, B. K.; McCarthy, J. F.; Parlange, J. Y. Capillary retention of colloids in unsaturated porous media. *Water Resour. Res.* **2008**, *44* (4), W04504.
- (29) Zevi, Y.; Gao, B.; Zhang, W.; Morales, V. L.; Cakmak, M. E.; Medrano, E. A.; Sang, W.; Steenhuis, T. S. Colloid retention at the meniscus-wall contact line in an open microchannel. *Water Res.* **2012**, *46* (2), 295–306.
- (30) Litton, G. M.; Olson, T. M. Colloid deposition rates on silica bed media and artifacts related to collector surface preparation methods. *Environ. Sci. Technol.* **1993**, *27* (1), 185–193.
- (31) Morales, V. L.; Gao, B.; Steenhuis, T. S. Grain surface-roughness effects on colloidal retention in the vadose zone. *Vadose Zone J.* **2009**, *8* (1), 11–20.
- (32) Zhang, W.; Morales, V. L.; Cakmak, M. E.; Salvucci, A. E.; Geohring, L. D.; Hay, A. G.; Parlange, J. Y.; Steenhuis, T. S. Colloid transport and retention in unsaturated porous media: effect of colloid input concentration. *Environ. Sci. Technol.* **2010**, *44* (13), 4965–4972.
- (33) Bradford, S. A.; Yates, S. R.; Bettahar, M.; Simunek, J. Physical factors affecting the transport and fate of colloids in saturated porous media. *Water Resour. Res.* **2002**, *38* (12), 1327.
- (34) Sang, W. J.; Morales, V. L.; Zhang, W.; Stooft, C. R.; Gao, B.; Schatz, A. L.; Zhang, Y. L.; Steenhuis, T. S. Quantification of Colloid Retention and Release by Straining and Energy Minima in Variably Saturated Porous Media. *Environ. Sci. Technol.* **2013**, *47* (15), 8256–8264.
- (35) Dobson, K. R.; Stephenson, M.; Greenfield, P. F.; Bell, P. R. F. Identification and treatability of organics in oil shale retort water. *Water Res.* **1985**, *19* (7), 849–856.
- (36) Mukherjee, B.; Weaver, J. W. Aggregation and charge behavior of metallic and nonmetallic nanoparticles in the presence of competing similarly-charged inorganic ions. *Environ. Sci. Technol.* **2010**, *44* (9), 3332–3338.
- (37) Brant, J.; Lecoanet, H.; Hotze, M.; Wiesner, M. Comparison of electrokinetic properties of colloidal fullerenes (n-C-60) formed using two procedures. *Environ. Sci. Technol.* **2005**, *39* (17), 6343–6351.
- (38) Moayedi, H.; Kazemian, S. Zeta Potentials of Suspended Humus in Multivalent Cationic Saline Solution and Its Effect on Electro-Osmosis Behavior. *J. Dispers. Sci. Technol.* **2013**, *34* (2), 283–294.
- (39) Bradford, S. A.; Torkzaban, S.; Walker, S. L. Coupling of physical and chemical mechanisms of colloid straining in saturated porous media. *Water Res.* **2007**, *41* (13), 3012–3024.
- (40) Bradford, S. A.; Simunek, J.; Walker, S. L. Transport and straining of E-coli O157: H7 in saturated porous media. *Water Resour. Res.* **2006**, *42* (12).
- (41) Redman, J. A.; Grant, S. B.; Olson, T. M.; Estes, M. K. Pathogen filtration, heterogeneity, and the potable reuse of wastewater. *Environ. Sci. Technol.* **2001**, *35* (9), 1798–1805.
- (42) Harter, T.; Wagner, S.; Atwill, E. R. Colloid transport and filtration of *Cryptosporidium parvum* in sandy soils and aquifer sediments. *Environ. Sci. Technol.* **2000**, *34* (1), 62–70.
- (43) Ramachandran, V.; Fogler, H. S. Multilayer deposition of stable colloidal particles during flow within cylindrical pores. *Langmuir* **1998**, *14* (16), 4435–4444.
- (44) Tong, M. P.; Ma, H. L.; Johnson, W. P. Funneling of flow into grain-to-grain contacts drives colloid-colloid aggregation in the presence of an energy barrier. *Environ. Sci. Technol.* **2008**, *42* (8), 2826–2832.
- (45) Bradford, S. A.; Simunek, J.; Bettahar, M.; van Genuchten, M. T.; Yates, S. R. Significance of straining in colloid deposition: Evidence and implications. *Water Resour. Res.* **2006**, *42* (12), W12S15.
- (46) Marmur, A. A kinetic theory approach to primary and secondary minimum coagulations and their combination. *J. Colloid Interface Sci.* **1979**, *72* (1), 41–48.
- (47) Hahn, M. W.; Abadzic, D.; O'Melia, C. R. Aquasols: On the role of secondary minima. *Environ. Sci. Technol.* **2004**, *38* (22), S915–S924.
- (48) Torkzaban, S.; Kim, H. N.; Simunek, J.; Bradford, S. A. Hysteresis of colloid retention and release in saturated porous media during transients in solution chemistry. *Environ. Sci. Technol.* **2010**, *44* (5), 1662–1669.
- (49) Shen, C.; Li, B.; Huang, Y.; Jin, Y. Kinetics of coupled primary- and secondary-minimum deposition of colloids under unfavorable chemical conditions. *Environ. Sci. Technol.* **2007**, *41* (20), 6976–6982.
- (50) Hahn, M. W.; O'Melia, C. R. Deposition and reentrainment of Brownian particles in porous media under unfavorable chemical conditions: Some concepts and applications. *Environ. Sci. Technol.* **2004**, *38* (1), 210–220.
- (51) Shen, C.; Huang, Y.; Li, B.; Jin, Y. Effects of solution chemistry on straining of colloids in porous media under unfavorable conditions. *Water Resour. Res.* **2008**, *44* (5), W05419.
- (52) Grolimund, D.; Borkovec, M. Release of colloidal particles in natural porous media by monovalent and divalent cations. *J. Contam. Hydrol.* **2006**, *87* (3–4), 155–175.
- (53) Chen, K. L.; Elimelech, M. Influence of humic acid on the aggregation kinetics of fullerene (C60) nanoparticles in monovalent and divalent electrolyte solutions. *J. Colloid Interface Sci.* **2007**, *309* (1), 126–134.
- (54) Torkzaban, S.; Wan, J. M.; Tokunaga, T. K.; Bradford, S. A. Impacts of bridging complexation on the transport of surface-modified nanoparticles in saturated sand. *J. Contam. Hydrol.* **2012**, *136*, 86–95.
- (55) Bradford, S. A.; Torkzaban, S.; Leij, F.; Šimunek, J.; van Genuchten, M. T. Modeling the coupled effects of pore space geometry and velocity on colloid transport and retention. *Water Resour. Res.* **2009**, *45* (2), W02414.
- (56) Tong, M.; Johnson, W. P. Colloid Population Heterogeneity Drives Hyperexponential Deviation from Classic Filtration Theory. *Environ. Sci. Technol.* **2006**, *41* (2), 493–499.
- (57) Ouali, L.; Pefferkorn, E. Fragmentation of Colloidal Aggregates Induced by Polymer Adsorption. *J. Colloid Interface Sci.* **1994**, *168* (2), 315–322.
- (58) Torkzaban, S.; Bradford, S. A.; Wan, J.; Tokunaga, T.; Masoudih, A. Release of Quantum Dot Nanoparticles in Porous Media: Role of Cation Exchange and Aging Time. *Environ. Sci. Technol.* **2013**, *47* (20), 11528–11536.
- (59) Smith, J. E.; Gillham, R. W. Effects of solute concentration-dependent surface tension on unsaturated flow: Laboratory sand column experiments. *Water Resour. Res.* **1999**, *35* (4), 973–982.
- (60) Haines, W. B. Studies in the physical properties of soils. V. The hysteresis effect in capillary properties, and the modes of water distribution associated therewith. *J. Agric. Sci.* **1930**, *20* (1), 97–116.
- (61) Pefferkorn, E. The role of polyelectrolytes in the stabilisation and destabilisation of colloids. *Adv. Colloid Interface Sci.* **1995**, *56* (0), 33–104.

- (62) Torkzaban, S.; Bradford, S. A.; Walker, S. L. Resolving the coupled effects of hydrodynamics and DLVO forces on colloid attachment in porous media. *Langmuir* **2007**, *23* (19), 9652–9660.
- (63) Bradford, S. A.; Torkzaban, S.; Wiegmann, A. Pore-scale simulations to determine the applied hydrodynamic torque and colloid immobilization. *Vadose Zone J.* **2011**, *10* (1), 252–261.
- (64) Crist, J. T.; Zevi, Y.; McCarthy, J. F.; Throop, J. A.; Steenhuis, T. S. Transport and retention mechanisms of colloids in partially saturated porous media. *Vadose Zone J.* **2005**, *4* (1), 184–195.